JOURNAL OF THERMOPHYSICS AND HEAT TRANSFER
Vol. 8, No. 4, Oct.–Dec. 1994

Evaporation from an Extended Meniscus for Nonisothermal Interfacial Conditions

K. P. Hallinan* and H. C. Chebaro†
University of Dayton, Dayton, Ohio 45469
S. J. Kim‡
IBM, Inc., Tucson, Arizona 85744
and
W. S. Chang§
Wright Laboratory, Wright-Patterson Air Force Base, Ohio 45433

A study is presented to determine the effects of evaporation from the thin film region of a liquid-vapor meniscus within the micropores of a heat pipe porous or grooved wick on the interfacial shape, temperature distribution, and pressure distribution. Wayner's theoretical treatment of evaporating thin films is applied to the problem of an evaporating extended meniscus within circular or slotted pores. In this application of Wayner's model, the nondimensional momentum equation is uniquely scaled in terms of the capillary number, to justify the use of the static meniscus curvature as a boundary condition for the extended meniscus profile even for the dynamic evaporating conditions studied herein. This boundary condition for small capillary numbers is consistent with the observation of the nearly constant meniscus curvature with evaporation rate that the thin film must asymptotically approach. From these basic tenets, the mechanical and thermal behavior of a stably, evaporating, nonisothermal extended meniscus is predicted. The resulting predictions are qualitatively consistent with the experimental findings of Wayner and the previous theoretical studies. They further support the claims that for the cases studied herein, both thermocapillary stresses and vapor recoil stresses at the liquid-vapor interface are negligible. However, scaling arguments are presented that identify the conditions necessary for these terms to be important.

Nomenclature

A = Hamaker constant
Ca = capillary number, $\mu_l u_0/\sigma$
C_1 = accommodation coefficient
h = film thickness
J = dimensionless grouping defining importance
K = curvature
k = liquid thermal conductivity
M = molecular weight
$\dot{m}_{evp}$ = evaporative mass flux
$\dot{m}_{id}$ = ideal evaporative flux
$\boldsymbol{n}$ = normal vector to liquid-vapor interface
P = pressure
R = radius or width of pore
R_g = universal gas constant
S = dimensionless grouping defining importance of thermocapillary stresses
T = temperature
u = velocity parallel to wall
$\boldsymbol{u}_v$ = vapor velocity
V = molar volume
X, Y = dimensionless groupings defining importance of circumferential curvature
x = axial spatial coordinate
y = spatial coordinate perpendicular to wall
Δh = latent heat of vaporization
η = dimensionless film thickness
θ = dimensionless temperature
κ = ratio of evaporative to conductive thermal resistance
μ = dynamic coefficient of friction
ξ = dimensionless axial coordinate
Π = disjoining pressure
ρ = density
σ = surface tension

Subscripts
a = pertaining to the transition region
I = pertaining to the interline region
l = liquid
v = vapor
0 = reference state

Received Dec. 16, 1993; revision received March 21, 1994; accepted for publication March 23, 1994.
*Professor of Mechanical Engineering.
†Research Associate.
‡Research Engineer, Thermal Engineering Center, SSD.
§Research Scientist. Member AIAA.

Introduction

IT has been postulated that the high heat transport rates exhibited by heat pipes are indebted to the process of thin film evaporation. The presence of the thin film as a region of the liquid-vapor interface within the micropores of a heat pipe wick (see Fig. 1) constitutes a transition between a flat nonevaporating adsorbed film, a microscopic region where the free energy of the liquid-vapor interface is dominated by the molecular potential between the fluid molecules at the liquid-vapor interface and the adjacent molecules of the solid wick, and the meniscus region, a macroscopic region dominated by the curvature of the liquid-vapor interface. Thus, the thin film is a region where the combined effects of the solid-fluid molecular interactions and the curvature of the liquid-vapor interface are important.

The analysis of the thin film thermofluid behavior is indebted to Derjaguin,[1] who showed that the gross effect of the solid-liquid molecular interactions on the liquid in the thin film is a pressure reduction relative to the pressure of the vapor phase in equilibrium with the thin film. This pressure

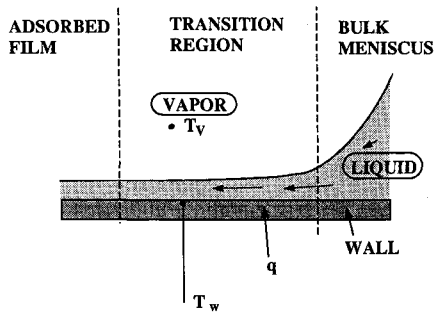

Fig. 1 Thin film region between an adsorbed film and a meniscus.

reduction was referred to as the disjoining pressure. For nonpolar fluids, a general theory of van der Waals forces was developed that was used to establish the relationship of the disjoining pressure to the local film thickness.[2,3]

Using the concept of the disjoining pressure, a continuum description of the thin film was made possible. Analysis of the evaporating thin film thermofluid behavior was established first by Derjaguin et al.,[4] and later more completely by Wayner et al.[5] In the latter studies of nearly perfectly wetting liquids, the thin film has been characterized as having small interfacial slope and Reynolds numbers, allowing for the application of boundary-layer type approximation to describe the fluid mechanics in the thin film region. Their results show that the interline heat transfer coefficient varies rapidly from zero at the adsorbed film, indicating zero evaporation at the adsorbed film, to a value equal to the overall interfacial heat transfer coefficient over a small distance from the adsorbed film, indicating that the choking effect of the disjoining pressure on the evaporation is confined to the near proximity of the adsorbed film. Moosman and Homsy[6] used a perturbation analysis to extend Wayner's theoretical treatment of the interline, to investigate the transport processes associated with a horizontal, evaporating, nonisothermal interface formed at the exit of two parallel plates. Their results likewise show that the evaporation rate profiles obtained for their geometry exhibit sharp peak values in the thin film region. Wayner and Schonberg[7,8] investigated the effect of varying evaporation rates on the interfacial shape of a liquid-vapor interface formed between the exits of two capillary feeders. Their results show that the thin film curvature approaches a constant asymptotic value as the thin film joins the meniscus. However, this asymptotic value of the thin film curvature in their geometry may increase with increasing evaporation rates.

Experimentally, Welter[9] studied the effect of evaporation on the interfacial shape in a capillary tube, where the liquid is resupplied to the interface solely by capillarity. He observed that for stable evaporating interfacial conditions a variation in the evaporation rate did not noticeably alter the radius of curvature of the meniscus region, which was observed to be equal to the radius of the capillary tube for the perfectly wetting liquids considered in his experiments. The significance of this result is that it indicates that for an evaporating interface within a capillary tube the thin film curvature approaches an asymptotic value equal to the invariant meniscus curvature, thereby imposing a boundary condition to the thin film interfacial shape as the thin film at its maximum extent.

Wayner et al.[10] used ellipsometry and interferometry to measure the thin film profile and the adsorbed film thickness for an evaporating interface formed at the exit of circular capillary feeder. Their results showed that the shape of the thin film in the interline region is only slightly tapered as it merges with the flat adsorbed film, and that the adsorbed film thickness decreases with increasing evaporation rate. These observations characterize the interfacial shape in proximity of the adsorbed film, and thus they define the interfacial thin film boundary conditions that must be satisfied in the proximity of the adsorbed film.

Relative to capillary resupplied evaporation from cylindrical or grooved pores such as exist in heat pipes, the effect of thin film evaporation on their performance was first addressed by Holm and Goplen.[11] Their results, obtained by neglecting the effect of interfacial curvature on the liquid in the thin film, indicated that roughly 80% of the evaporative heat transport of heat pipes utilizing triangular capillary grooves occurs in the thin film. More recently, Stephan and Busse[12] predicted similar trends in an extension of Holm and Goplen's analysis to account for the conjugate heat transfer problem, associated with both the heat pipe wall and the liquid within the groove, and by accounting for the effect of interfacial curvature in the thin film. Swanson and Herdt[13] considered the evaporation process from the liquid-vapor interface within the micropores of a heat pipe porous wick under nonisothermal interfacial conditions. They assumed a Hagen-Poiseuille flowfield for the liquid in the meniscus and thin film regions, and solved for the entire liquid-vapor interfacial shape. The results of their study uniquely show that the mean curvature of the meniscus region is constant, a result that is experimentally confirmed by Welter.[9] Finally, Chebaro and Hallinan[14] considered the same geometry as Swanson and Herdt,[13] but for isothermal interfacial conditions. Their approach was to compute only the thin film region interfacial shape, while imposing on the thin film interfacial shape the condition that its asymptotic curvature must be equal to the invariant curvature of the meniscus region consistent with the pore geometry. One result of this study was to show that the thin film region may sustain increasing evaporation rates by decreasing in length and thickness. The decrease in the thin film length and thickness occurs in order to increase the liquid flow rate from the base of the meniscus to the thin film. However, the assumption of isothermal interfacial conditions in this study is unrealistic, as this assumption causes the evaporation rate to peak in the meniscus region instead of the thin film.

The goal of the current study is to extend the study of Chebaro and Hallinan[14] to consider the more realistic nonisothermal evaporating extended meniscus that merges with the bulk or intrinsic meniscus in circular or slotted pores. The present analysis applies the approach of Schonberg and Wayner[8] to the capillary pore geometry. It also utilizes the same reasoning for selecting the thin film boundary conditions as described in Chebaro and Hallinan[15] for the nonisothermal problem. Uniquely, the momentum equation is scaled in terms of Ca to justify the use of the static meniscus curvature as a boundary condition for the extended meniscus profile even for the dynamic conditions studied herein, where there is evaporation from the extended meniscus. Scaling arguments are presented to justify the use of a Cartesian frame of reference for circular pores, except for very small pore radii, and to justify the neglect of thermocapillary and vapor recoil stresses at the liquid-vapor interface.

Analysis

The thin liquid film between the adsorbed film and the meniscus of an evaporating interface is considered under nonisothermal conditions. A rectangular coordinate frame of reference is employed, with the x axis along the wall, and the y axis normal to the wall as depicted in Fig. 1, where $x = 0$ at the intersection of the adsorbed film with the thin film. The use of an x-y coordinate system neglects the circumferential curvature which, as shown by Dussan et al.,[16] is insignificant at least in determining the flowfield for the length scales considered within the thin film region. The conditions that must be present in order to insure the appropriateness of this assumption are described later. The thin film region is characterized for wetting liquids, typical of those used in most heat pipes, by small interfacial slope, and hence, as shown from a dimensional analysis by Moosman and Homsy,[6] the viscous stresses normal to the interface are negligible relative to surface tension and disjoining pressure in determining the capillary pressure $P_v - P_i$. The interfacial tangential stress is

also assumed negligible, and thus the interface is said to be "mobile."[17] Furthermore, for small Reynolds and Bond numbers typical of micropores, the inertial forces normal to the interface, due mostly to the vapor recoil, are also small. Thus, the normal stress equation is reduced to the augmented Laplace-Young equation equation

$$P_v - P_l = \sigma K + \Pi \tag{1}$$

where P_v is the vapor pressure and P_l is the liquid pressure. Note that, by neglecting the tangential stress due to a surface tension gradient and using Eq. (1) for the interfacial normal stress balance, the results from this analysis will represent a base solution for assessing the effects of the interfacial vapor recoil and thermocapillary stresses.

The evaporation model of Wayner et al.,[5] which is indebted to the synthesis of condensation and evaporation data by Schrage[18] and modified to account for the effects of curvature and disjoining pressure on the evaporation rate for small differences in temperature between the interface and the vapor, is used here and is given by

$$\dot{m}_{\text{evp}} = C_1 \left(\frac{M}{2\pi R_g T_{lv}}\right)^{1/2} \times \left[\frac{P_v M \Delta h}{R_g T_v T_{lv}} (T_{lv} - T_v) + \frac{V_l P_v}{R_g T_{lv}} (P_l - P_v)\right] \tag{2}$$

where M is the molar mass of the fluid, T_v is the temperature of the vapor, T_{lv} is the interfacial liquid temperature, and V_l is the molar volume.

The dynamics of the liquid flow in the thin film are approximated by the lubrication theory of fluid mechanics and as a boundary layer-type approximation, hence

$$\mu_l \frac{\partial^2 u}{\partial y^2} = \frac{dP_l}{dx} \tag{3}$$

where $p_l = P_l(x)$. Utilizing a no shear stress condition at $y = h$, $(\partial u/\partial y) = 0$, which assumes a negligible surface tension gradient at the interface, and a no slip condition at the wall, $u = 0$, Eq. (3) is solved, yielding

$$u(y) = \frac{1}{\mu_l} \frac{dP_l}{dx} \left(\frac{y^2}{2} - hy\right) \tag{4}$$

The validity of the assumption of a negligible surface tension gradient will be addressed later.

Using the velocity profile given by Eq. (4), the mass flow rate across an area of height h and unit width is given by

$$\Gamma = \frac{\rho_l}{\mu_l} \frac{dP_l}{dx} \int_0^h \left(\frac{y^2}{2} - hy\right) dy = -\frac{h^3}{3\nu_l} \frac{dP_l}{dx} \tag{5}$$

Assuming that the pressure field in the vapor phase is constant and differentiating Eq. (1) with respect to x, gives a relationship for dP_l/dx as shown:

$$\frac{dP_l}{dx} \simeq -\frac{d}{dx} (\sigma K + \Pi) \tag{6}$$

where for the small slope approximation

$$K \simeq \frac{d^2 h}{dx^2} \tag{7}$$

Strictly, this expression for the curvature is valid only for a slotted pore, but can be shown to be approximately valid for circular pores. More accurately, for a circular pore the curvature is

$$K = \left\{ \frac{1}{r_i \left[1 + \left(\frac{dr_i}{dx}\right)^2\right]^{1/2}} - \frac{\frac{d^2 r_i}{dx^2}}{\left[1 + \left(\frac{dr_i}{dx}\right)^2\right]^{3/2}} \right\} \tag{8}$$

where r_i is the radial distance from the tube center to the liquid-vapor interface. Scaling arguments can be used to justify the approximation for the curvature in Eq. (7), and therefore justify the use of a Cartesian frame of reference, especially as the difference between the wall temperature and the vapor temperature increases. The Cartesian frame of reference is argued to be a reasonable approximation if 1) the circumferential curvature term leads to a negligible change in pressure drop in the extended meniscus relative to the axial curvature term; and 2) the contribution of the circumferential curvature has a negligible effect on the film profile in the extended meniscus. The conditions necessary for ensuring these two requirements are developed below.

The circular pore curvature defined in Eq. (8) in the extended meniscus where the film slope is small is approximated as, using $h = R - r_i$:

$$K \approx \left(\frac{1}{R - h} + \frac{d^2 h}{dx^2}\right) \tag{9}$$

The flowfield in the extended meniscus occurs as a result of the axial pressure gradient, dP_l/dx defined in Eq. (6). Substituting the above expression for K into this equation yields

$$\frac{dP_l}{dx} = \frac{d\Pi}{dx} + \sigma \left[\frac{\frac{dh}{dx}}{(R - h)^2} + \frac{d^3 h}{dx^3}\right] \tag{10}$$

If the second term in the curvature expression is much smaller than the first, then the change in circumferential curvature has a negligible contribution on the flowfield. Using h_0 and x_0 as reference length scales, this condition requires for $R >> h$ that

$$(x_0/R)^2 << 1 \tag{11}$$

The axial length scale x_0 is selected to represent the length of the extended meniscus at which the capillary pressure term balances the disjoining pressure term

$$x_0 \sim (\sigma h_0/\Pi_0) \tag{12}$$

where Π_0 is the reference disjoining pressure A/h_0^3. Finally, the reference film thickness h_0, for the worst case scenario, is maximally given by the equilibrium adsorbed film thickness, obtained from a balance of the disjoining pressure in the adsorbed film with the capillary pressure in the intrinsic meniscus:

$$h_0 \sim (AR/\sigma) \tag{13}$$

Then, from Eqs. (11–13), in order for the circumferential curvature gradient to have a negligible effect on the flowfield in the extended meniscus, the following inequality must be satisfied:

$$X = (A/\sigma R^2)^{1/3} << 1 \tag{14}$$

Given approximate values of the modified Hamaker constant, $A \sim 10^{-21} J$ and $\sigma \sim 0.01$ N/m, the pore radius must be much greater than 10^{-9} m. Clearly, pore radii greater than 0.1 μm ensure this requirement.

To ensure that the circumferential radius of curvature likewise has negligible effect on the film thickness, the circumferential curvature must also have a negligible effect on the adsorbed film thickness, which can be inferred by recognizing that by definition the adsorbed film has zero evaporation rate. Therefore, from Eq. (2), using

$$a = C_1\left(\frac{M}{2\pi R_g T_{lv}}\right)^{1/2}\frac{P_v M\Delta h}{R_g T_v T_{lv}}$$
$$b = C_1\left(\frac{M}{2\pi R_g T_{lv}}\right)^{1/2}\frac{V_l P_v}{R_g T_{lv}} \tag{15}$$

and the augmented Laplace-Young equation to express $P_l - P_v$, and further assuming that $T_{lv} \approx T_w$ in the adsorbed film, then

$$(a/b)(T_w - T_v) - \Pi_0 - \sigma K_0 = 0 \tag{16}$$

Above, K_0 is the adsorbed film curvature $1/R$. If the curvature term is to have a negligible contribution on the adsorbed film thickness, then from Eq. (16)

$$Y = \frac{\sigma/R}{(a/b)\Delta T} << 1 \tag{17}$$

This dimensionless grouping represents the ratio of the capillary pressure difference between the extended meniscus and the adsorbed film to the pressure drop in the extended meniscus. When the pressure drop due to the flow is large, the circumferential term has a negligible contribution to the adsorbed film thickness. That such a situation is possible is apparent from the experimental observations of Sujani and Wayner,[19] who showed that only small temperature differences (1 mK) are only necessary to dramatically affect the adsorbed film thickness.

Assuming that the inequalities given by Eqs. (14) and (17) are satisfied, the use of a Cartesian frame of reference is henceforth considered valid. The analysis then proceeds by applying conservation of mass within the film. This requires that the reduction in the liquid flow rate equals the evaporation rate, thus

$$\frac{d\Gamma}{dx} = \dot{m}_{evp} \tag{18}$$

For nonisothermal conditions, the evaporative flux will depend locally upon the interface temperature. Thus, in addition to solving for the flow and pressure fields, it is also necessary to solve the energy equation for the temperature field. Neglecting advective heat transport and axial conduction, and assuming that the wick wall temperature, T_w is approximately constant, the energy equation reduces to

$$\frac{d^2T}{dy^2} = 0 \tag{19}$$

The boundary conditions needed to solve Eq. (19) are given by

$$T(0) = T_w \quad \text{and} \quad -k\left.\frac{dT}{dy}\right|_{y=h} = \dot{m}_{evp}\Delta h$$

Utilizing these boundary conditions, Eq. (19) is solved yielding

$$T(y) = (\dot{m}_{evp}\Delta h/k)y + T_w \tag{20}$$

Low-temperature heat pipe wicks are manufactured out of metals such as copper, aluminum, or stainless steel, which possess much higher thermal conductivities than the working liquids used in heat pipes. As a result, the transport of energy through the walls of the wick should yield minimal temperature drop, and therefore T_w is approximately constant and is assumed to be approximately the same as the temperature of the heat source. This claim has been previously substantiated by temperature measurements of Holm and Goplen[11] along the wall of a triangular groove.

The temperature of the interface along the thin film $T_{lv}(x)$ is obtained by substituting h for y in Eq. (20), yielding

$$T_{lv} = (\dot{m}_{evp}\Delta h/k)h + T_w \tag{21}$$

The following nondimensional variables are now defined:

$$\eta = h/h_0, \quad \xi = x/x_0, \quad \Pi^* = \Pi/\Pi_0$$
$$\dot{m}_{id} = \rho_l u_0, \quad Ca = \mu_l u_0/\sigma, \quad x_0 = (\sigma h_0/\Pi_0)^{1/2}$$
$$\dot{m}_{id} = C_1\left(\frac{M}{2\Pi R_g T}\right)^{1/2}\left[\frac{P_v M\Delta h}{R_g T_v T_{lv}}(T_w - T_v)\right]$$
$$\Pi_0 = \frac{M\Delta h\Delta T_0}{V_l T_v}, \quad \Delta T_0 = T_w - T_v$$
$$\theta = \frac{T_{lv} - T_v}{T_w - T_v}, \quad \kappa = \frac{\Delta h\dot{m}_{id}}{(k/h_0)}$$

where u_0 is a characteristic velocity of the liquid, and κ represents the ratio of evaporative interfacial resistance to conductive resistance in the thin film.

The combination of Eqs. (1), (2), and (21) yield a relationship for the nondimensional interfacial temperature θ in terms of the nondimensional film thickness η given by

$$\theta = \frac{\Delta T_0 + \kappa(\eta\eta'' + \eta\Pi^*)}{\Delta T_0 + \kappa\eta} \tag{22}$$

In obtaining Eq. (22), the product $T_{lv}T_v$ and T, which is given by $\frac{1}{2}(T_{lv} + T_v)$ in Eq. (2), are approximated as T_v^2 and T_v, respectively. Now, combining Eqs. (18) and (22), the following nondimensional fourth-order ordinary differential equation for the thin film interfacial shape is obtained

$$-[\eta^3\eta''' + \eta^3(\Pi^*)']' = \frac{3Ca}{(h_0\Pi_0/\sigma)^2}\left[\frac{\Delta T_0 + \kappa(\eta\eta'' + \eta\Pi^*)}{\Delta T_0 + \kappa\eta} - \eta'' - \Pi^*\right] \tag{23}$$

The choice of the capillary number, defined as the ratio of viscous to surface tension forces in the intrinsic or bulk meniscus, as a dimensionless parameter is that its magnitude helps to identify the boundary condition for the extended meniscus for large film thicknesses (where the extended meniscus merges with the intrinsic meniscus). This dimensionless variable has been used in the related topic of advancing/receding menisci in capillaries to correlate the increase in the apparent contact angle θ_d for dynamic conditions. In general, the correlation has been of the form[20,21]:

$$\theta_d = \theta_d[Ca, F(\theta_s)] \tag{24}$$

where $F(\theta_s)$ is some function of the static contact angle. Generally, it has been shown that the dynamic contact angle changes negligibly relative to the static angle when $Ca < 10^{-5}$.

The problem of evaporation from a stationary meniscus parallels that of an advancing meniscus where the meniscus is fixed in space, but where the tube wall is drawn downward at a velocity u. Therefore, the magnitude of the capillary number can be used to assess whether the contact angle increases dynamically, and therefore, in a pore geometry, how the intrinsic meniscus curvature changes relative to static equi-

librium curvature. (If the contact angle increases, then the bulk curvature must decrease.) The capillary numbers typical of phase change devices relying upon evaporation from pores are generally much smaller than 10^{-5}. Thus, the intrinsic meniscus curvature for dynamic evaporating conditions is approximately equal to that for static equilibrium conditions, as has been observed by Welter.[9]

The procedure that will be used to solve Eq. (23) for the thin film interfacial profile employs the same procedure developed by Chebaro and Hallinan[15] in studying an evaporating thin film within micropores under isothermal interfacial conditions. The boundary conditions needed to solve Eq. (23) are to be specified in a manner that forces the asymptotic curvature of the thin film to match the curvature of the meniscus. Ideally, the other boundary conditions would be specified at the adsorbed film according to $\eta = \eta_0$ and $\eta' = \eta'' = \eta''' = 0$. However, because the resulting solution is strictly the adsorbed film solution, $\eta = \eta_0 = \text{const}$, it is necessary to specify the boundary conditions at a point shifted away from the adsorbed film ($\xi = \xi_a$), where ξ_a will be chosen with the requirement that at ξ_a, η_a'' is negligibly small, and $\eta_a''' \simeq 0$. Thus, in general form the following boundary conditions at $\xi = \xi_a$ are employed:

$$\eta = \eta_a, \qquad \eta' = \eta_a', \qquad \eta'' = \eta_a'' \qquad \text{and} \qquad \eta_a''' = 0$$

The condition imposed on the choice of ξ_a guarantees that ξ_a belongs to the so-called interline region, the region of the thin film where the interfacial curvature is negligible. Since the interline region or region adjacent to the adsorbed film is characterized by negligible curvature, the differential equation that governs its interfacial profile is obtained by setting the curvature terms in Eq. (12) to zero,[5] yielding the following equation:

$$-[\eta_l^3(\Pi_l^*)']' = \frac{3Ca}{(h_0\Pi_0/\sigma)^2}\left(\frac{\Delta T_0 + \kappa\eta_l\Pi_l^*}{\Delta T_0 + \kappa\eta_l} - \Pi_l^*\right) \qquad (25)$$

valid in the region $0 \le \xi \le \xi_a$. The boundary conditions for Eq. (25) are chosen to be consistent with the contention of Dussan et al.[16] just outside the adsorbed film, i.e.,

$$\eta_l = 1 + \delta \qquad \text{and} \qquad \eta_l' = \varepsilon \qquad \text{at} \qquad \xi \simeq 0$$

The parameter δ depends on the evaporation rate as shown in Wayner's experiments. The interline slope ε has been postulated by Dussan to be fluid-solid dependent only,[16] and independent of the thin film and the meniscus region. Thus, prescription of these boundary conditions may be sufficient to describe the physical boundary conditions inherent to the thin film, although to obtain other than qualitative results the material value for ε must be obtained by experiment.

From the interline solution a matching point ξ_a is selected such that η_a'' will be negligibly small, but not zero, and at which the film thickness $\eta_l(\xi_a)$ and slope $\eta_l'(\xi_a)$ provide two of the initial conditions for the solution to Eq. (23) for the transition region, i.e., the remainder of the thin film region. Next, iteration is required upon η_a'' to obtain matching of the thin film asymptotic curvature with that of the meniscus.

The solutions of Eqs. (23) and (25) requires the specification of the form for Π. For organic fluids typical of low-temperature heat pipes, the contributions to Π are primarily van der Waal's forces, and thus the form of $\Pi = A/h^3$ is chosen. Using Gregory's approach for computing the effects of adhesion[22] A_{sl}, and using the combining relation described by Israelchvili[23] to account for effects of cohesion A_{ll}, a value for A of 3.18e − 19 was determined.

Results

Results are presented for a heat pipe utilizing ammonia as a working fluid and transporting heat between a sink and a source at a nearly constant source temperature of 50°C. The vapor temperature in the evaporator is assumed to be approximately the same as the temperature of the source. The heat pipe wick is considered to have an average pore radius of 20 μm. The average meniscus radius in the evaporator section will also be 20 μm that corresponds to an average meniscus curvature of 50,000/m. The evaporator heat transport rate of the heat pipe is a variable, while still maintaining the 50°C average operating temperature by adjusting the heat sink conditions. For differences between the wall temperature and the vapor temperature, $\Delta T = T_w - T_v$, of 0.0015, 0.002, and 0.0025 K, the corresponding average heat transport rates for the thin film portion of the interface only (i.e., the transport from the meniscus region is found to be negligible) are respectively, 0.206, 0.405, and 0.55 W/cm^2. These heat fluxes are obtained by multiplying the latent heat of vaporization by the average evaporation rate from the extended meniscus.

For these heat fluxes the following interline boundary conditions are used:

$\bar{q}'' = 0.203$ W/cm^2

$$\xi = 0.00, \quad \eta_l = 1.04, \quad \eta_l' = 0.0001$$

$\bar{q}'' = 0.405$ W/cm^2

$$\xi = 0.00, \quad \eta_l = 1.04, \quad \eta_l' = 0.0001$$

$\bar{q}'' = 0.550$ W/cm^2

$$\xi = 0.00, \quad \eta_l = 1.04, \quad \eta_l' = 0.0001$$

At ξ_a, iteration upon η_a'' to obtain matching with the meniscus region yields the following boundary conditions for the thin film region:

$\bar{q}'' = 0.203$ W/cm^2

$$\xi_a = 53.6, \quad \eta = 1.21, \quad \eta' = 0.01373, \quad \eta'' = 0.0009027$$

$\bar{q}'' = 0.405$ W/cm^2

$$\xi_a = 40.8, \quad \eta = 1.25, \quad \eta' = 0.01565, \quad \eta'' = 0.0010231$$

$\bar{q}'' = 0.550$ W/cm^2

$$\xi_a = 38.0, \quad \eta = 1.30, \quad \eta' = 0.01883, \quad \eta'' = 0.0012071$$

The choice of these boundary conditions is obtained through iteration, to insure that the "initial conditions" near the adsorbed film yield an interfacial curvature that equals the static equilibrium meniscus curvature outside of the transition region. The interline slope η_l' is selected to be constant at a specified value of η_l, consistent with the "material slope" hypothesis of Dussan.[16] The values for each of these were selected primarily to ensure the stability of the numerical technique. As the heat flux was increased, the length of the transition region decreases, thus the value of ξ_a at which the interline region is matched to the transition region decreases.

The subsequent solution to Eqs. (23) and (25) yields data for interfacial shape, evaporative flux, pressure distribution, and interfacial temperature distribution within the thin film. Figure 2 shows three thin film profiles computed for ammonia for the above heat transport rates. The profiles shown in the figure are the combined solution of Eqs. (23) and (25). This figure indicates a decrease in the film length with increasing heat fluxes and also shows that in the bulk or intrinsic meniscus region the small slope approximation is still valid ($dh/dx < 0.2$). Figure 3 provides an exploded view of the thin films in the interline region, which clearly shows that the thickness of the adsorbed film decreases with increasing heat transport rates. For a different geometry (i.e., a capillary

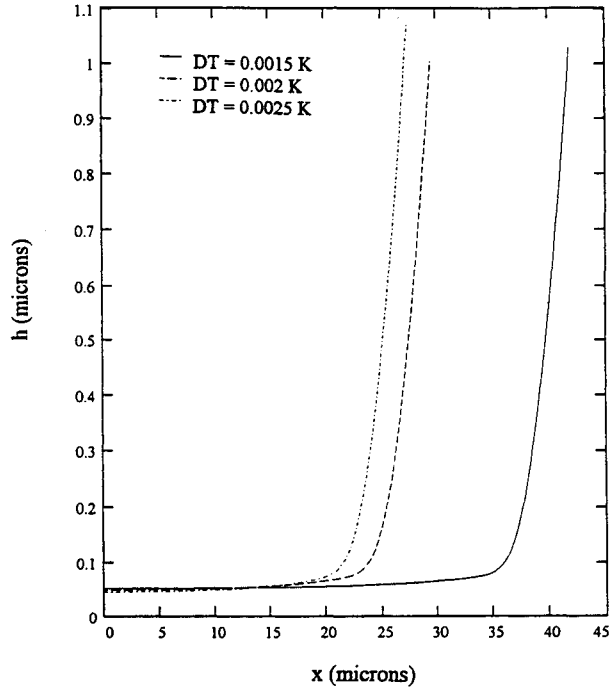

Fig. 2 Thin film profiles for ammonia at vapor temperature of 322 K.

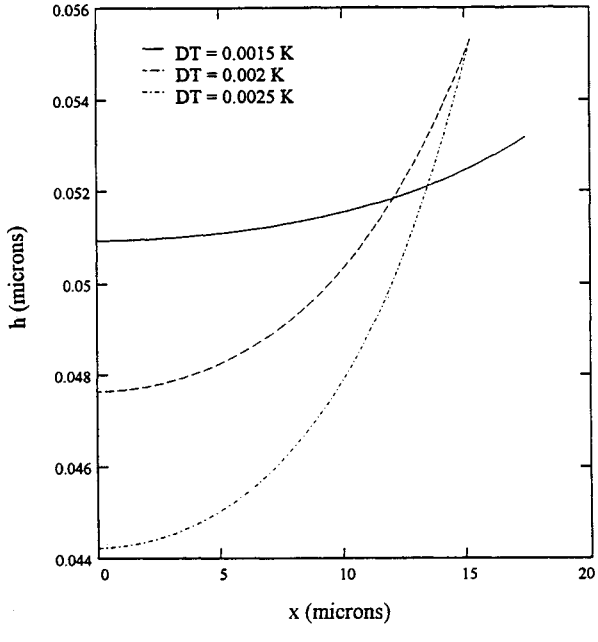

Fig. 3 Exploded view of the thin film profiles in the proximity of the adsorbed film.

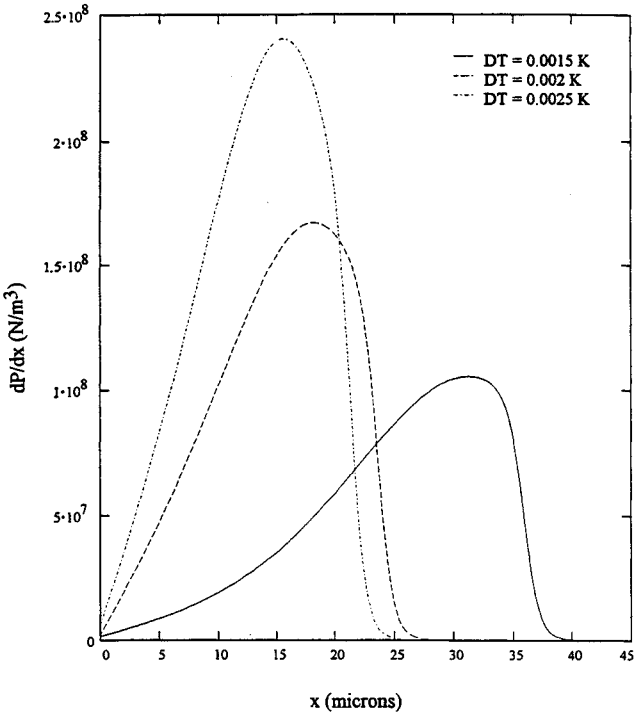

Fig. 4 Evaporation profiles for ammonia at vapor temperature of 322 K.

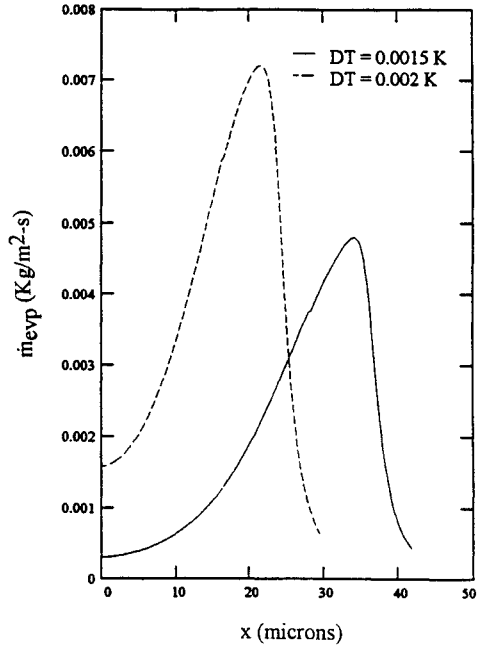

Fig. 5 Pressure gradient profiles for ammonia at vapor temperature 322 K.

feeder where experimentally the meniscus curvature is not constrained by a tiny pore geometry), Wayner and co-workers[10] experimentally verified the same trend using ellipsometry to measure the adsorbed film thickness. The decrease in the film length and thickness with increasing heat transport rate is due to an associated increase in the evaporative fluxes as seen in Fig. 4. When the evaporation increases from the thin film, the liquid flow rate from the base of the meniscus to the thin film has to increase in order to maintain steady-state operation. This can occur only by increasing the pressure gradient in the liquid (see Fig. 5). The liquid pressure in the meniscus or curvature-controlled region is unaffected by the evaporation rate since the meniscus curvature is constant. Thus, in order to supply increasing flow rates to the thin film region with increasing evaporation rate, the pressure gradient must increase, and the liquid pressure in the thin film and the length of the thin film must decrease. The adsorbed film thickness must also decrease, as with increasing evaporation rates in the thin film the total pressure drop from the meniscus region to the adsorbed film increases. This is achieved by increasing the disjoining pressure (A/h_0^3) in the adsorbed film. Therefore, the adsorbed film thickness h_0 must decrease.

For a 20-μm pore, Fig. 4 shows that the evaporation from the liquid-vapor interface in the proximity of the meniscus is small. However, because the surface area is large, the total evaporation from the meniscus region is likely dominant, and thus no conclusion can be made about the relative importance of the thin film evaporation relative to the total evaporation from the meniscus. The figure also shows that the evaporation

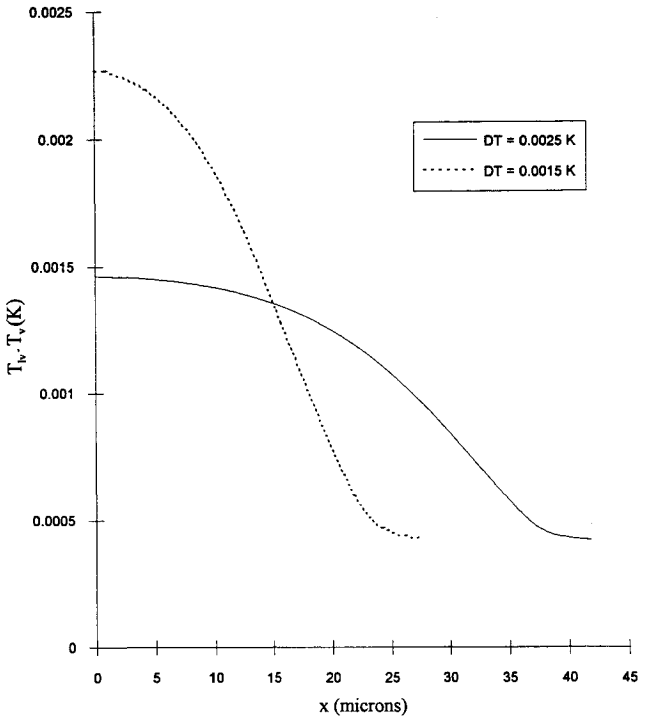

Fig. 6 Thin film temperature distribution for ammonia at vapor temperature of 322 K.

from the interface reaches a maximum in the thin film. Figure 6 shows the interfacial temperature variation for $\Delta T = 0.0015$ and 0.0025 K. Obvious from this figure is that for the low average heat fluxes considered, the interfacial temperature variation is extremely small.

The results of this study were obtained by neglecting thermocapillary stresses and vapor recoil stresses at the liquid-vapor interface in the extended meniscus. That these assumptions are valid for the conditions studied is evident from the following scaling arguments. Significant interfacial thermocapillary stresses would require that the tangential shear stress boundary condition at $y = h$ for small slope be

$$\mu \left.\frac{\partial u}{\partial y}\right|_{y=h} = \frac{d\sigma}{dx} \tag{26}$$

With this boundary condition, the solution of Eq. (3) for the the velocity field is

$$u = \frac{1}{\mu}\left[\frac{dP_l}{dx}\left(\frac{y^2}{2} - hy\right) + \gamma \frac{dT_{lv}}{dx} y\right] \tag{27}$$

where γ is equal to $d\sigma/dT$. In the extended meniscus, $dP_l/dx \sim d\Pi/dx$, therefore, in order for thermocapillary stresses to be neglected, the thermocapillary stress term must be significantly lower in magnitude than the disjoining pressure gradient term. After scaling each term, the following criterion defining the conditions required for the neglect of thermocapillary stresses to be reasonable is established:

$$\Pi_0(h_0/x_0) >> \gamma \Delta T(h_0/x_0) \tag{28}$$

or

$$S = (\gamma \Delta T/\Pi_0 h_0) << 1 \tag{29}$$

Here, S represents the ratio of the thermocapillary force acting on the extended meniscus to the disjoining pressure potential. Since $\Pi_0 \sim A/h_0^3$, and, as discussed previously, $h_0 \sim (AR/\sigma)^{1/3}$, this inequality can be rewritten as

$$S = (\gamma \Delta T R^{2/3}/A^{1/3}\sigma^{2/3}) << 1 \tag{30}$$

Table 1 Numerical values of important dimensionless groupings

	$\bar{q}_w = 0.208$ W/cm^2	$\bar{q}_w = 0.403$ W/cm^2	$\bar{q}_w = 0.550$ W/cm^2
1) X	5.31376	3.985	3.188
Y	4.87e − 6	4.87e − 6	4.87e − 6
2) Ca	8.2e − 7	1.1e − 6	1.38e − 5
3) S	0.0087	0.01162	0.0145
4) J	0.3e − 7	1.4e − 6	2.25e − 6

Interestingly, this requirement shows that thermocapillary stresses become more important as R, ΔT, and γ increase, and diminish for higher cohesion and adhesion forces (σ and A, respectively). These trends are expected.

Vapor recoil stresses in the extended meniscus are maximum since the local evaporative flux is greatest there. Neglecting them implies that their contribution in the normal stress balance is small relative to the disjoining and capillary pressures, i.e.,

$$\rho_v \boldsymbol{u}_v \cdot \boldsymbol{n} << \Pi_0 \tag{31}$$

Scaling each of these terms and rearranging, the above inequality can be written as

$$J = (\rho_l/\rho_v)(\rho_l u_0^2 R/\sigma) << 1 \tag{32}$$

This requirement demonstrates that vapor recoil stresses become more significant as surface tension effects are diminished with increasing pore size.

Table 1 summarizes the magnitudes of the dimensionless grouping for the three cases studied that are important for justifying 1) the use of a Cartesian frame of reference (X, Y); 2) the assumption that the intrinsic meniscus curvature is unchanged from the static curvature (Ca); 3) that thermocapillary stresses are negligible (S); and 4) that vapor recoil stresses are negligible (J).

That Y is much less than 1 for each of the cases guarantees that the flowfield, and therefore pressure drop, is unaffected by the gradient of the circumferential curvature. This likewise implies that the meniscus shape is unaffected by the neglect of the circumferential curvature. At the same time, it is also apparent that X is not small, indicating that the predicted adsorbed film thickness is slightly smaller than had the exact curvature been considered. (The difference, however, is no more than 20% greater.) That the capillary number for each case is substantially less than 10^{-5} justifies the assumed static equilibrium intrinsic meniscus curvature as a boundary condition for the extended meniscus for dynamic evaporating conditions. That S and J are likewise much less than 1 justifies the neglect of thermocapillary and vapor recoil stresses. However, it should be noted that for $\bar{q}_w = 0.403$ W/cm^2, the magnitude of S is such that the neglect of thermocapillary stresses at the liquid-vapor interface may not precisely describe the thermofluid physics in the thin film.

Conclusions

The results of the study indicate, as expected, that maximum evaporative fluxes from the wall-heated meniscus are present in the extended meniscus when constant wall temperature, and therefore nonisothermal interfacial conditions, are considered. Furthermore, this study has shown how different evaporation rates, and therefore, evaporator heat fluxes, can be sustained at the same heat pipe saturation conditions (i.e., the same operating temperature). Since the base meniscus curvature is set by the standard pore curvature of the wick, which is unchanged with increasing evaporation rates for small capillary numbers, then in order to sustain higher evaporation rates, the extended meniscus must adjust by decreasing in length to help increase the pressure gradient, and by decreasing the thickness of the adsorbed film, with the same result.

These results show that ever increasing evaporation rates can be stably maintained simply by the shortening of the thin film and by decreasing the adsorbed film thickness. Such a situation is not feasible, for the stability of the thin film in sustaining evaporation is a big concern. With increasing heat flux, the thin film interfacial temperature gradient increases, thereby increasing the relative importance of thermocapillary stresses on the interface. These thermocapillary stresses may ultimately choke the flow into the thin film and, as such, must be investigated more completely.

The results have also demonstrated that the magnitude of the interfacial tangential stress and the interfacial vapor recoil are small. However, despite the small magnitude of these disturbances, the thin film region could become unstable subject to such disturbances,[24] with instabilities arising similar to the above mechanism.[25]

References

[1]Derjaguin, B. V., "A Theory of Capillary Condensation in the Pores of Sorbents and of Other Capillary Phenomena Taking into Account the Disjoining Action of Polymolecular Liquid Films," *Acta Physicochimica* (USSR), Vol. 12, No. 1, 1940, pp. 181–200.

[2]Dzyaloshinskii, I. E., Lifshitz, E. M., and Pitaevskii, L. P., "The General Theory of Van der Waals Forces," *Advances in Physics*, Vol. 10, No. 38, 1961, pp. 165–209.

[3]Verwey, E. J. W., and Overbeek, J. Th. G., *Theory of the Stability of Lyophobic Colloids*, Elsevier, Amsterdam, 1948.

[4]Derjaguin, B. V., Nerpin, S. V., and Churaev, N. V., "Effect of Film Transfer upon Evaporating Liquids from Capillaries," *RILEM Bulletin*, Vol. 29, No. 1, 1965, pp. 93–98.

[5]Wayner, P. C., Jr., Kao, Y. K., and Lacroix, L. V., "The Interline Heat Transfer Coefficient of an Evaporating Wetting Film," *International Journal of Heat and Mass Transfer*, Vol. 19, No. 2, 1976, pp. 487–492.

[6]Moosman, S., and Homsy, G. M., "Evaporating Menisci of Wetting Fluids," *Journal of Colloid and Interface Sciences*, Vol. 73, No. 1, 1980, pp. 212–223.

[7]Wayner, P. C., Jr., and Schonberg, J. F., "Heat Transfer and Fluid Flow in an Evaporating Extended Meniscus," 9th International Heat Transfer Conf., Israel, 1990.

[8]Schonberg, J. A., and Wayner, P. C., Jr., "Analytical Solution for the Integral Contact Line Evaporative Heat Sink," *Journal of Thermophysics and Heat Transfer*, Vol. 6, No. 1, 1992, pp. 128–134.

[9]Welter, D., "The Effect of Evaporation on the Dynamic Capillary Pressure in Heat Pipes," M.S.M.E. Thesis, Univ. of Dayton, Dayton, OH, 1991.

[10]Wayner, P. C., Jr., DasGupta, S., and Schonberg, J. F., "Effect of Interfacial Forces on Evaporative Heat Transfer in a Meniscus," WL-TR-91–2061, Wright-Patterson AFB, OH, 1991.

[11]Holm, F. W., and Goplen, S. P., "Heat Transfer in the Meniscus Thin-Film Transition Region," *Journal of Heat Transfer*, Vol. 101, Aug. 1979, pp. 543–546.

[12]Stephan, P. C., and Busse, C. A., "Theoretical Study of an Evaporating Meniscus in a Triangular Groove," 7th International Heat Pipe Conf., Minsk, USSR, 1990.

[13]Swanson, L. W., and Herdt, G. C., " Model of the Evaporating Meniscus in a Capillary Tube," *Journal of Heat Transfer*, Vol. 114, May 1992, pp. 434–441.

[14]Chebaro, H. S., Hallinan, K. P., Kim, S. J., and Chang, W. S., "Evaporation from a Porous Wick Heat Pipe for Isothermal Interfacial Conditions," Winter Annual Meeting of the American Society of Mechanical Engineers, Anaheim, CA, Nov. 1992.

[15]Chebaro, H. S., and Hallinan, K. P., "Boundary Conditions for an Evaporating Thin Film for Isothermal Interfacial Conditions," *Journal of Heat Transfer*, Vol. 115, Aug. 1993, pp. 816–819.

[16]Dussan, V. E. B., Rame, E., and Garoff, S., " On Identifying Boundary Conditions at a Moving Contact Line: An Experimental Investigation," *Journal of Fluid Mechanics*, Vol. 230, Sept. 1991, pp. 97–116.

[17]Lin, C. Y., and Slattery, J. C., "Thinning of a Liquid Film as a Small Drop or Bubble Approaches a Solid Plane," *AIChE Journal*, Vol. 28, No. 1, 1982, pp. 147–156.

[18]Schrage, R. W., *A Theoretical Study of Interphase Mass Transfer*, Columbia Univ. Press, New York, 1953.

[19]Sujani, M., and Wayner, P. C., Jr., "Microcomputer-Enhanced Optical Investigation of Transport Processes with Phase Change in Near-Equilibrium Thin Liquid Films," *Journal of Colloid and Interface Sciences*, Vol. 143, No. 2, 1991, pp. 472–488.

[20]Hoffman, R. L., "A Study of the Advancing Interface I. Interface Shape in Liquid-Gas Systems," *Journal of Colloid and Interface Sciences*, Vol. 50, No. 2, 1975, pp. 228–240.

[21]Hoffman, R. L., "A Study of the Advancing Interface II. Theoretical Prediction of the Dynamic Contact Angle in Liquid-Gas Systems," *Journal of Colloid and Interface Sciences*, Vol. 94, No. 2, 1983, pp. 470–486.

[22]Gregory, J., "The Calculation of Hamkaer Constants," *Advances in Colloid and Interface Science*, Vol. 2, No. 2, 1969, pp. 396–417.

[23]Israelchavili, J. N., *Intermolecular and Surface Forces*, Academic Press, New York, 1989.

[24]Ruckenstein, E., and Jain, R., "Spontaneous Rupture of Thin Liquid Films," *Journal of the Chemical Society Faraday Transactions II*, Vol. 70, No. 1, 1973, pp. 132–147.

[25]Palmer, H. J., "The Hydrodynamic Stability of Rapidly Evaporating Liquids at Reduced Pressure," *Journal of Fluid Mechanics*, Vol. 75, Pt. 3, 1976, pp. 487–511.